2024 Design, Automation & Test in Europe Conference (DATE 2024)
Special Initiative "Autonomous Systems Design"

An Adaptive UAV Scheduling Process to Address Dynamic Mobile Network Demand Efficiently

Ruide Cao[1,6], Jiao Ye[2], Jin Zhang[3,5], Qian You[1], Chao Tang[4], Yan Liu[1,5,6], Yi Wang*[1,5,6]
[1]Institute of Future Networks, [3]Department of Computer Science and Engineering, [4]School of Design, SUSTech
[2]School of Architecture and Urban Planning, SZU [5]Peng Cheng Laboratory [6]DET of Heyuan

***Abstract*—Benefiting from high flexibility and probability of line-of-sight, deploying unmanned aerial vehicles (UAVs) as aerial access points has emerged as a promising solution for ensuring reliable wireless connectivity in crowded events. This paper introduces a UAV scheduling process adaptive to dynamic mobile network demand, including three phases. In the sensing phase, the user distribution is sensed, and user number thresholds are set to determine whether UAV assistance is needed. The planning phase presents an enhanced mean shift algorithm to find suitable locations to deploy UAVs with a dynamic bandwidth derived from the user distribution, the UAV's maximum capacity, and the UAV's maximum throughput. The deploying phase dispatches and recalls UAVs based on planning results. Comprehensive simulation experiments are conducted on OMNeT++ using real-world data. Results show that the proposed process shows great adaptivity, with an efficiency increase of 18.7% and a fairness increase of 28.9% compared to the existing related works on average.**

I. Introduction

Recently, unmanned aircraft systems (UAS) have been proven more cost-efficient than conventional terrestrial infrastructure in more and more scenarios [1]–[3]. Due to their high deployment flexibility, UAS have displayed substantial promise across a spectrum of applications, expanding from military to civilian. One of the most attractive applications is using UAS to assist mobile network communications.

Mobile network demand in cities is dramatically dynamic on both spatial and temporal scales. Although the ground base stations (GBSs) nowadays can adapt to the users through beamforming and power control, they can not meet the demand cost-efficiently due to their immobility. Unmanned aerial vehicles (UAVs) can be quickly deployed to target locations to provide extra network coverage and capacity. Therefore, heterogeneous networks incorporating UAVs as relays or aerial base stations (ABSs) to augment terrestrial network infrastructure have become the subject of extensive discussion [4]. Among them, one of the critical issues is the 2D deployment of UAVs.

Similar to the GBS location problem mentioned in [5], UAV deployment is a case of the (metric) uncapacitated facility location problem (UFLP), which is known to be NP-hard. The exact optimal solutions are only available in small-scale situations. Hence, many studies designed rules, reinforcement learning (RL) algorithms, and heuristics to find near-optimal solutions for real-world UFLP instances. For an example of rules, [6] suggested an *circle packing in a circle* deployment scheme based on the circle packing theory, and [7] proposed a ring-pattern solution. These rule-based approaches only work as predefined and have no adaptation to the environment.

*Corresponding author: Yi Wang (wy@ieee.org).
Map information from OpenStreetMap (openstreetmap.org/copyright).

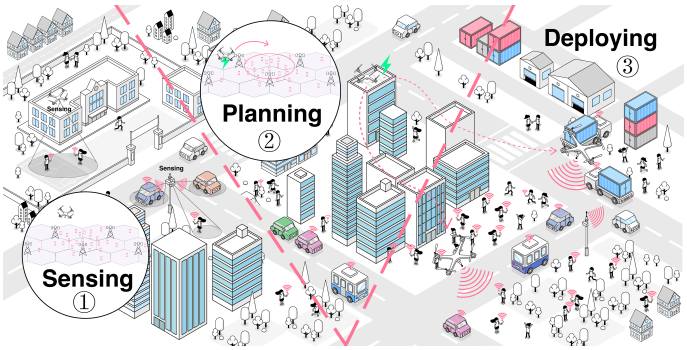

Fig. 1. Overview of the adaptive UAV scheduling process.

RL models can adapt to evolving environments through continuous learning. [8] designed a Q-learning algorithm for a single ABS. The effectiveness was well demonstrated in a comparison of 19 GBSs versus 18 GBSs plus 1 ABS. [9] then constructed a deep Q-learning framework for multiple ABSs, with a simulation validation performed in sudden traffic scenario. [10] further proposed an ABS placement optimization method based on double deep Q-learning which can notably increase user coverage rate. However, as pointed out in [11], the major problem with applying RL is the lack of field data. While RL models can adapt to the environment, they require accurate perceptions of complex environmental states, enormous computational resources, and long inference time. Consequently, RL approaches face cost limitations in meeting the real-time demands of dynamic scenarios.

Compared to RL, heuristics are less data-dependent and more applicable to real-world instances. K-means is the most widely used heuristic technique to cluster the ground users (GUs) and plan the target locations of the UAVs. A key issue in applying the k-means is how to set the k value, which is the number of clusters. [12] fix the k value to the number of users divided by the UAV capacity rounded downwards, while [13] set k to the unsatisfiable throughput demand divided by the throughput a UAV can provide. In [14], a lower bound on the spacing between the UAVs is suggested. So k keeps shrinking in successive attempts until this spacing constraint is satisfied. These strategies consider the UAVs' capacity limit, throughput limit, and spacing limit, respectively, and may lead to different k values. The adaptivity of k-means approaches is limited since there is no way for the joint consideration of

979-8-3503-4859-0/DATE24/© 2024 EDAA

multiple constraints to be realized by only one k.

As a non-parametric heuristic technique, mean shift can autonomously derive the clusters based on kernel density estimation without prior assuming numbers or shapes on data clusters. [15] first suggested applying the mean shift technique to classify GUs in the UAV deployment problem with an Epanechnikov kernel. [16] also proposed a UAV planning strategy based on mean shift. However, these efforts both use a fixed kernel function bandwidth, which can lead to the over-shift problem, where the UAV deployment location is always shifted to where the crowd density is the highest, and the surrounding GUs are not covered. In addition, they focus merely on providing signal coverage to GUs without further considering whether a UAV could meet the demand of all the GUs it covered. Moreover, most of the above works considered deployment in static scenarios without bridging between two successive deployments in dynamic scenarios.

In this paper, an adaptive UAV scheduling process consisting of three phases is proposed. In the sensing phase, the UAV collaborates with the GBSs to sense the dynamic distribution of target GUs. In the planning phase, the deployment scheme is planned based on the sensed GU distribution. In the deployment phase, the assignment problem between UAVs and target locations is solved by applying the Hungarian algorithm. This process extends the aforementioned static deployment approaches into dynamic scheduling by introducing time slots and repeating these three phases at each time slot.

Driven by the observation of real-world GU travel patterns and mobile network demand situations, an enhanced mean shift heuristic algorithm with dynamic bandwidth for UAV planning is designed. This algorithm integrates multiple constraints into account, including the UAVs' coverage, the UAVs' network capacity (in link number), and the throughput they can provide (in bps) so that it can adapt well to the evolving environment. Comprehensive real-time simulations are then conducted using a large-scale, high-dynamism, real-world dataset.

II. System Model

Let the UAV deployment scheme be updated with a fixed period. We define the time interval between two successive deployment schemes as a **time slot**. Without loss of generality, we set the time slot to begin at t_0 while ending at t_1 with a length of $\Delta t = t_1 - t_0$ and consider the following contents within a single time slot. All UAVs are assumed identical in our model, which means they work at the same altitude H with the same transmit power P^{tx} and coverage radius R. Interference between UAVs can be circumvented by staggering the signal frequencies and deploying them in a cellular fashion. Collisions can be avoided from the UAS design perspective. Thus, they are not discussed here.

Having more than 1 GUs in the user set $\mathcal{U}$, we use $\mathbf{u}_i(t) = [x_{u_i}(t), y_{u_i}(t)]^{\mathrm{T}}$ to represent the 2D coordinate of the ith GU in $\mathcal{U}$ at time t. Each GU selects the UAV that provides the maximum throughput for connectivity. Although these UAVs are identical, it does not mean that the closer the UAV is, the higher the throughput. For a GU, when the nearer UAV has reached its maximum backhaul throughput T_{max}, choosing a more distant UAV to connect might bring greater throughput. We use $\mathbf{n}_i(t) = [x_{n_i}(t), y_{n_i}(t)]^{\mathrm{T}}$ to denote the UAV in $\mathcal{N}$ that can best serve $\mathbf{u}_i(t)$ at time t. Then we have

$$d_i(t) = \sqrt{\|\mathbf{u}_i(t) - \mathbf{n}_i(t)\|_2^2 + H^2}, \tag{1}$$

for the Euclidean distance between $\mathbf{u}_i(t)$ and $\mathbf{n}_i(t)$, where $\|\cdot\|_2$ indicates the ℓ_2 norm, and

$$\phi_i(t) = \arccos(\frac{H}{d_i(t)}), \tag{2}$$

for the down angle from $\mathbf{n}_i(t)$ to $\mathbf{u}_i(t)$.

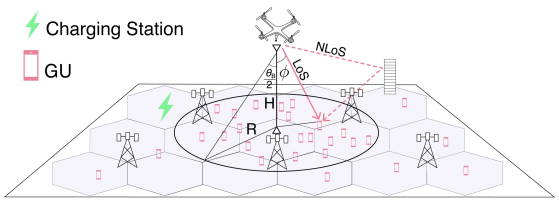

Fig. 2. System model.

The beam-forming technique can concentrate energy on the main lobe to enhance the signal while suppressing side lobes to minimize interference in other directions. We assume that all UAVs are equipped with vertical antennas that support beam-forming and only serve GUs in their main lobe. According to [6], [17], the directional antenna gain is approximated with

$$G = \begin{cases} G_0, & \phi \le \frac{\theta_B}{2}, \\ g(\phi), & \text{otherwise}, \end{cases} \tag{3}$$

where $G_0 \approx \frac{29000}{\theta_B^2}$, θ_B is in degrees, and $g(\phi)$ is negligible.

The probability of having a line-of-sight (LoS) link between $\mathbf{u}_i(t)$ and $\mathbf{n}_i(t)$ is considered in line with [18], as

$$PLoS_{u_i}(t) = \frac{1}{1 + \vartheta \exp(-\xi(90 - \phi_i(t)) - \vartheta)}, \tag{4}$$

and the free-space path loss is

$$FSPL_{u_i}(t) = 20 \log(\frac{4\pi f_c d_i(t)}{c}). \tag{5}$$

Then, the overall path loss can be calculated using

$$PL(dB) = FSPL + PLoS * \eta_{LoS} + PNLoS * \eta_{NLoS}, \tag{6}$$

where $PNLoS = 1 - PLoS$, η_{LoS} and η_{NLoS} denote the additional loss for LoS and NLoS connections. We then have the ideal throughput of $\mathbf{u}_i$ at time t as:

$$R_{u_i}(t) = Blog_2(1 + \frac{P_{u_i}^{rx}(t)}{N}), \tag{7}$$

where $P_{u_i}^{rx}(t) = P^{tx} + G - PL_{u_i}(t)$ is the received signal power of $\mathbf{u}_i(t)$ from $\mathbf{n}_i(t)$. Note that this value may need to be scaled down in a proportion of $T_{max}/R_{n_i}(t)$ since the total throughput $R_{n_i}(t)$ offered to GUs by $\mathbf{n}_i(t)$ never exceeds the maximum throughput of its backhaul link. Consequently, we have the total throughput of $\mathbf{u}_i$ within a time slot in bits:

$$T_{u_i} = \int_{t_0}^{t_1} \min(1, \frac{T_{max}}{R_{n_i}(t)}) * R_{u_i}(t)\, dt. \tag{8}$$

Finally, we use the following two metrics to assess the deployment schemes in our model holistically:

Metric 1: While radio-frequency power for data transmission varies from 0.01W to 10W [15], [19], the mechanical power of a standard-size UAV is usually above 100W [20], [21]. Since mechanical power dominates the consumed power on UAVs, this paper models the energy consumption by $N\Delta t$, which is the flight time of UAVs. We define the efficiency index as

$$\textit{Efficiency Index} := \frac{\sum_{u_i}^{U} T_{u_i}}{|\mathcal{N}|\Delta t\, T_{max}}. \tag{9}$$

Metric 2: The Jain's fairness index [22], which is widely used to evaluate how fair a system allocates its resources to the users, is given by

$$\textit{Fairness Index} := \frac{(\sum_{u_i}^{U} T_{u_i})^2}{|\mathcal{U}| \sum_{u_i}^{U} T_{u_i}^2} \tag{10}$$

III. UAV Scheduling Process Design

To adaptively address the dynamic demand, we propose an adaptive UAV scheduling process (Alg. 1) with three phases: a *sensing phase* (lines 3-11), a *planning phase* (lines 13-14), and a *deploying phase* (lines 15-21). The structure of this section is organized accordingly.

Algorithm 1 UAV Scheduling Process

1: $\mathcal{C}_{over} \leftarrow \{\}$; $t_0 \leftarrow$ start time; $t_1 \leftarrow t_0 + \Delta t$
2: **while** $t_0 \leq t < t_1$ **do**
3: **for** each GBS cell C **do**
4: **if** C not in $\mathcal{C}_{over}$ **and** $L_C \geq L * f_{on}$ **then**
5: Insert C into $\mathcal{C}_{over}$
6: **else if** C in $\mathcal{C}_{over}$ **and** $L_C \leq L * f_{off}$ **then**
7: Remove C from $\mathcal{C}_{over}$
8: **end if**
9: **end for**
10: $\mathcal{U} \leftarrow$ all GUs located by the UAS and GBSs
11: $\mathcal{U}' \leftarrow \mathcal{U} \in \mathcal{C}_{over}$
12: **if** $\mathcal{U}' \neq \emptyset$ **then**
13: Successive mean shift clustering over $\mathcal{U}'$ with Alg. 2
14: $\mathcal{T} \leftarrow$ 2D locations of the cluster centers
15: **if** $|\mathcal{T}| > |\mathcal{N}|$ **then**
16: Insert $\mathbf{c}$ into $\mathcal{N}_{list}$ for $|\mathcal{T}| - |\mathcal{N}|$ times
17: **else if** $|\mathcal{T}| < |\mathcal{N}|$ **then**
18: Insert $\mathbf{c}$ into $\mathcal{T}_{list}$ for $|\mathcal{N}| - |\mathcal{T}|$ times
19: **end if**
20: Matching $\mathcal{T}_{list}$ and $\mathcal{N}_{list}$ by the Hungarian algorithm
21: Deploying UAVs according to the matching result
22: **end if**
23: Wait till $t_1 \leq t$; $t_0 \leftarrow t_1$; $t_1 \leftarrow t_0 + \Delta t$
24: **end while**

A. Sensing Phase

With accurate localization of GUs can be accomplished by 5G GBSs [23], we consider each GBS cell to have a capacity limit L. Only when the number of GUs within a cell exceeds $L * f_{on}$ is the cell an overloading cell till the GU number falls back to $L * f_{off}$ or less. All GUs in the overloading cells $\mathcal{C}_{over}$ are target GUs. Both f_{on} and f_{off} should be smaller than 1. We intentionally set a gap between them to let f_{on} slightly larger than f_{off}. By this gap, GU number jitter near the borderlines does not cause a cell to flip between normal and overloading repeatedly in adjacent time slots. The sensing phase then gives a more stable target GU distribution input to the subsequent planning phase, which ultimately favors the stability of the deployment schemes.

B. Planning Phase

Algorithm 2 Mean Shift with Adaptive Bandwidth

Input : GU set $\mathcal{U}'$
Output: Target location set $\mathcal{T}$
1: $\lambda = 0$, $\mathcal{T} = \{\}$
2: $n = \min(C_{max} * f_n,\ |\mathcal{U}'|) - 1$
3: **for** $\mathbf{u}_i$ in $\mathcal{U}'$ **do**
4: $\mathbf{u}_{i,n} \leftarrow$ the n-th neighbor of $\mathbf{u}_i$ in $\mathcal{U}'$
5: $\lambda \mathrel{+}= \|\mathbf{u}_i - \mathbf{u}_{i,n}\|_2^2$
6: **end for**
7: $\lambda = \max(R * (1 - f_b), \min(R * (1 + f_b), \frac{\lambda}{|\mathcal{U}'|}))$
8: **for** $\mathbf{u}_i$ in $\mathcal{U}'$ **do**
9: Shift an ROI from u_i to the peak with kernel K_λ
10: **if** a UAV at the ROI center covers more than l GUs in $\mathcal{U}'$ **then**
11: $\mathcal{N}_i \leftarrow$ the 1st to $C_{max} - 1$th neighbors of $\mathbf{u}_i$ in $\mathcal{U}'$
12: $\mathcal{C}_i \leftarrow$ all GUs may covered by the UAV at the ROI center
13: Insert the ROI center location into $\mathcal{T}$
14: Remove $\mathbf{u}_i$ and GUs in $\mathcal{N}_i \cap \mathcal{C}_i$ from $\mathcal{U}'$
15: **end if**
16: **end for**
17: **return** $\mathcal{T}$

The enhanced mean shift with adaptive bandwidth for UAV planning is shown in Alg. 2. First, a suitable bandwidth is estimated as the average distance between $\mathbf{u}_i$ and its n-th neighbor (lines 1-7). Considering the limited capacity and throughput of a UAV, its actual service area might be smaller than its coverage area. We compensated the difference between the actual service area and the coverage area by the factor f_n while selecting the appropriate bandwidth, which scales up the UAV capacity C_{max} to a neighbor number n. At the same time, we use factor f_b to ensure that the estimated bandwidth only fluctuates within a specific range, thus avoiding extreme cases where too much or too little bandwidth leads to anomalies. Adaptation factors f_n, f_b work together to make the bandwidth adaptively float within a specific range. Intuitively, as the crowd becomes progressively denser, the dynamically estimated bandwidth will become progressively smaller, producing more clustering for more UAV deployments and thus providing better network services.

Second, we initialize a region-of-interest (ROI) on $\mathbf{u}_i$ and repeatedly shift the ROI towards the more crowded direction till convergence, and determine whether to deploy a UAV based on whether it can serve enough users at the ROI center. (lines 8-10). By setting a lower bound l of the serving GU number, we make the trade-off between efficiency and fairness more tractable. If we expect to save costs by increasing the efficiency of the UAV mobile network assistance service, we increase l, and the planning algorithm will respond to our needs. In practice, the value of l should be considered in terms of the cost-efficiency requirements of the actual deployment.

Third, once a UAV is added to the target location set $\mathcal{T}$, all GUs it can serve are excluded from subsequent consideration (lines 11-14). Doing so dramatically improves the efficiency of the algorithm in the first place. Although it does not change the theoretical computational complexity of the algorithm in the worst case, it effectively reduces the size of subsequent problems due to each valid deployment. Moreover, the problem of over-shift is solved because those who have already been served will no longer affect subsequent deployments. And finally, the target locations are returned as the input of the deployment phase (line 17).

C. Deploying Phase

After getting the target locations in the planning phase, how to assign them to the UAVs such that the total flight distance is minimized turns out to be a problem for successive deployments. We first supplement the charging station location $\mathbf{c}$ to the smaller list among $\mathcal{T}_{list}$ and $\mathcal{N}_{list}$ to ensure they are the same size. We can then formulate it as a bipartite graph with a layer of n UAV vertices and a layer of n target location vertices. These two layers are fully connected. Every edge linking a UAV vertex to a target location vertex has a cost that equals the distance between them. We finally add the constraint that the two layers of vertices must be matched one-to-one (perfect matching). Applying the Hungarian algorithm can lead us to the best assignment with minimum cost in polynomial time.

IV. Evaluation

For evaluation, an autonomous UAS consisting of multiple UAVs and a charging/scheduling center is constructed in OMNeT++, a discrete event simulator widely used for simulating various network systems. The proposed adaptive UAV scheduling process is then implemented on the UAS, with our proposed mean shift with adaptive bandwidth and other state-of-the-art algorithms implemented in the planning phase. Real-world data is collected and imported into the simulation environment, and comprehensive real-time simulations are performed. Data preprocessing and numerical results statistics were aided with MATLAB and Python language.

A. Benchmark

Our proposed mean shift algorithm with adaptive bandwidth (*MS-A*) is compared among *CPT* [6], *Ring* [7], *SD-KM* [14], k-means with the k adaptive to the number of target GUs (*KM-A*) [12], and mean shift with fixed bandwidth (*MS-F*) as mentioned in [15]. In CPT, we deploy 16 UAVs uniformly at fixed locations. For Ring, 5 UAVs follow concentric circle trajectories with different radii, maintaining a fixed angular difference of 72°. The minimum allowed spacing distance between two UAVs is set to R in SD-KM. Also, the bandwidth of MS-F is fixed to R. The k value in KM-A is set to the number of target GUs divided by C_{max} rounded down. In MS-A, the adaptation factors f_n, f_b are set to 1.38, 0.40, and the cluster lower bound l is set to 450.

With sufficient data, the choice of kernel function has little effect on the clustering results [24]. Our experiments verify this, as shown in Fig. 3. The flat kernel is used in MS-F and MS-A for simplicity and efficiency. Denoting the bandwidth as λ, we have the flat kernel:

$$K_\lambda(x) = \begin{cases} \frac{1}{\lambda^2}, & \|x\|_2^2 \le \lambda, \\ 0, & \text{otherwise}, \end{cases} \tag{11}$$

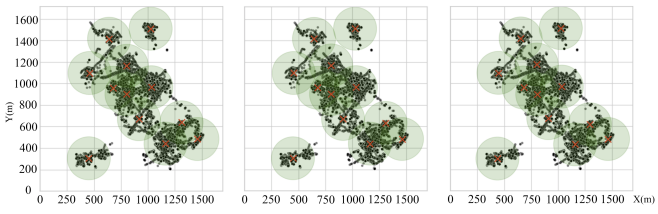

(a) Flat (b) Gaussian (c) Epanechnikov

Fig. 3. Planning results with the same bandwidth ($\lambda = 130\ m$) but different kernel functions. It takes a meticulous look to spot the tiny differences. One of the differences is the overlapping area of the uppermost two circles.

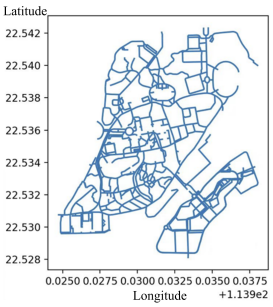

Fig. 4. Study area road map.

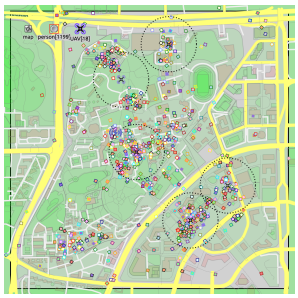

Fig. 5. OMNeT++ simulation scenario.

In addition to comparing the planning algorithms in static scenarios (a single time slot snapshot), we extend them to scheduling processes correspondingly: *CPTS, RingS, SD-KMS, KM-AS, MS-FS*, and *MS-AS*. The performance of these scheduling processes is observed and compared over a continuous period containing multiple time slots.

B. Dataset & Parameters

We take Shenzhen University Yuehai Campus as the study area, which accommodates over 48,000 students, faculty, and staff in an area of 2.72 km^2. The mobile network demand here is highly dynamic, with distinct peaks and valleys. Fig. 4 shows its road map. We use a dataset of 1400 person-days GPS logs recorded every 10 seconds from 7:00 to 24:00 on campus for our simulation experiments. Refer to [8], [25], the simulation parameters are shown in Table I. For consistency, we preferentially set the maximum throughput of a UAV to T_{max} and then derived its maximum capacity C_{max} based on the minimum VoIP call throughput (12.2 kbps) [26].

TABLE I
Simulation Parameters

Parameter	Symbol	Value	Parameter	Symbol	Value
Cell side length	-	100 m	Cell factors	f_{on}, f_{off}	0.90, 0.88
Cell capacity	L	180 links	LoS further losses	η_{LoS}	1.60
Coverage Radius	R	200 m	NLoS further losses	η_{NLoS}	23.0
UAV altitude	H	120 m	Urban Environment	ϑ, ξ	12, 0.14
Time slot length	Δt	300 s	Transmission power	P^{tx}	23 dBm
Noise power	N	-96 dBm	Backhaul throughput	T_{max}	30 Mbps
Signal frequency	f_c	2.0 GHz	UAV Capacity	C_{max}	2500 links
Bandwidth	B	15 MHz	Antenna Beamwidth	θ_B	118.1°
GU lower bound	l	450	Adaptation factors	f_n, f_b	1.38, 0.40

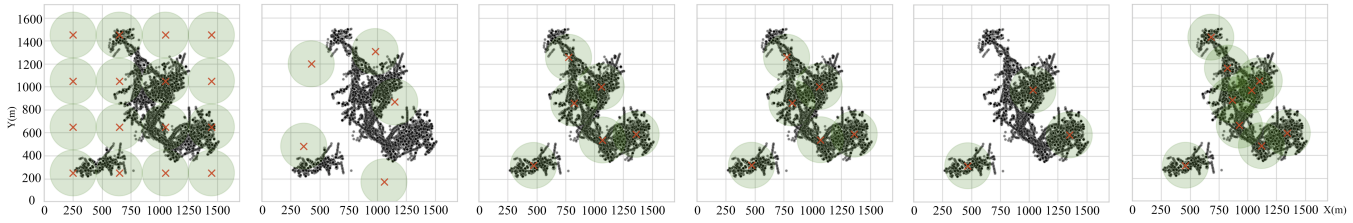

(a) CPT (b) Ring (c) SD-KM (d) KM-A (e) MS-F (f) MS-A (proposed)

Fig. 6. Deployment schemes planned at 12:30.

C. Simulation Results

Fig. 6 shows the deployment schemes generated by all the planning algorithms in the midday rush hour. CPT and Ring deploy UAVs according to predetermined rules, and neither demonstrates adaptivity. SDKM and KM-A generated similar deployment schemes because both set the k to 6 for k-means clustering, where SDKM is chosen based on the minimum spacing constraint for UAV, and KM-A is chosen based on the number of target users. Neither of these two deployment schemes dispatched enough UAVs to provide adequate network services.

As shown in Fig. 6(e), when the GU distribution is connected and there is a significant density difference, the ROI always shifts from the lower-density area to the higher-density area and converges to the highest-density area. Such an over-shift leads to the abandonment of GUs in the lower-density area. Suffering from the over-shift problem, MS-F dispatched only three UAVs, which was far from adequate. MS-A overcomes the over-shift problem by intelligently shrinking bandwidth when crowds are dense and excluding users that the UAV can serve after each deployment from consideration for subsequent deployments. MS-A shows sufficient adaptivity by deploying adequate UAVs at a suitable density in accurate locations.

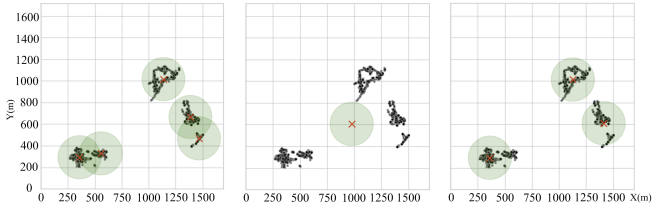

(a) SD-KM (b) KM-A (c) MS-A

Fig. 7. Deployment schemes planned at 23:30.

Fig. 7 shows late-night KM-A, SD-KM, and MS-A deployment schemes. Unlike during rush hours, the number of targeted GUs is low, and GUs are more dispersed. While MS-A performed ideally, SD-KM deployed more UAVs than required based on its minimum spacing constraint, resulting in low efficiency. KM-A deployed only one UAV since the demand was low, but it did not consider the dispersion of GUs, ultimately leading to a waste of resources.

The variation of throughput and GU number over time is illustrated in Fig. 8. CPTS provided enough throughput at times, but this comes at the cost of intensive deployment

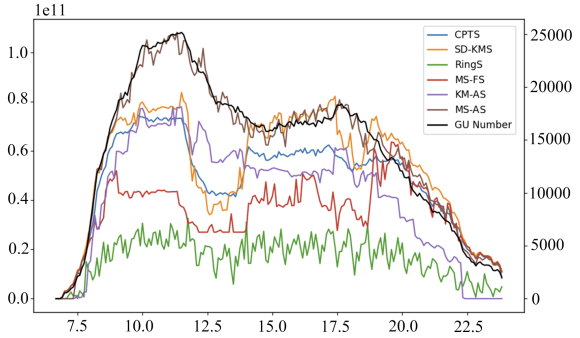

Fig. 8. Throughput and GU number versus time. The horizontal axis denotes time in hours, the primary vertical axis illustrates the corresponding throughput in bits, and the secondary vertical axis represents the number of target GUs.

throughout the day. RingS kept circling around the center of the area, and its throughput showed an apparent periodicity. At peak hours, GUs congregate so densely that CPTS and RingS cannot meet the demand by providing ubiquitous coverage. All heuristic-based scheduling processes show adaptivity, but only our proposed MS-AS adapted well to both peak and valley. SD-KM's spacing constraint prevents SD-KMS from making denser deployments. MS-FS also failed for dense deployment due to the over-shift problem of MS-F. So SD-KMS and MS-FS could not provide sufficient network capacity during the midday peak when the crowd density was the highest. KM-AS is able to provide sufficient network capacity during peak hours because the number of UAVs to be dispatched is determined by the number of target GU in KM-A. However, KM-AS cannot adapt to the GU distribution during the valley.

TABLE II
PERFORMANCE FROM 12:00 TO 14:00

	CPTS	RingS	SD-KMS	KM-AS	MS-FS	MS-AS
Throughput (Gb)	1083	416.5	1005	1453	671.1	1975
Flight Time (hour)	32.0	10.0	9.92	14.8	6.92	21.8
Efficiency	0.313	0.386	0.938	0.912	0.898	0.838
Fairness	0.602	0.227	0.705	0.814	0.667	0.932

TABLE III
PERFORMANCE FROM 22:00 TO 24:00

	CPTS	RingS	SD-KMS	KM-AS	MS-FS	MS-AS
Throughput (Gb)	470.4	129.4	499.3	79.06	470.1	460.3
Flight Time (hour)	32.0	10.0	10.4	2.42	8.00	6.75
Efficiency	0.136	0.120	0.444	0.303	0.544	0.631
Fairness	0.957	0.267	0.993	0.160	0.941	0.922

Table II and Table III show the performance of the different scheduling processes during the midday peak and the evening valley, respectively. During the peak, MS-AS provided the

highest throughput and the best fairness, indicating that it can provide high-quality network service during rush hours. Comes to the valley, MS-AS demonstrates the best efficiency since it did not invest excess resources in such a low-demand situation.

TABLE IV
OVERALL PERFORMANCE FROM 7:00 TO 24:00

	CPTS	RingS	SD-KMS	KM-AS	MS-FS	MS-AS
Throughput (Tb)	9.922	3.424	11.13	8.667	7.257	12.85
Flight Time (hour)	272.0	85.00	141.9	90.33	94.08	149.7
Efficiency	0.338	0.373	0.726	0.888	0.714	0.795
Fairness	0.724	0.253	0.841	0.735	0.613	0.922

The overall numerical results are shown in Table IV. Heuristic scheduling has significant advantages over rule-based scheduling. MS-AS provided the most network throughput and outperformed all the benchmarks on both efficiency and fairness, except for the efficiency of KM-AS. While only 9.3% less efficient than KM-A, MS-A provides 48.3% more throughput and is 18.7% better than KM-A in terms of fairness.

V. CONCLUSION

In conclusion, this paper has introduced a novel approach for addressing the challenges of adaptively, efficiently, and fairly supporting dynamic mobile network demand by deploying UAVs. We first design a three-phase iterative UAV scheduling process that autonomously 1) senses the target GU distribution, 2) plans the target locations of UAVs, and 3) deploys UAVs to assist GUs in accessing the mobile network. We then proposed an enhanced mean shift algorithm in the planning phase that dynamically selects the bandwidth based on the current GU distribution, considering the UAV's maximum coverage, maximum capacity, and maximum throughput. We conducted real-time simulations using real-world collected data to compare with the state-of-the-art algorithms. Results show that our proposed scheduling process improves efficiency by 18.7% and fairness by 28.9% compared to other processes' average performance. The proposed algorithm showcases exceptional adaptivity.

ACKNOWLEDGMENT

This work is supported by the National Key Research and Development Program of China (2020YFB1806400), the Major Key Project of Peng Cheng Laboratory (PCL2023AS2-3).

REFERENCES

[1] M. Virgili, N. Babu, M. Javidsharifi, I. Valiulahi, C. Masouros, A. J. Forsyth, T. Kerekes, and C. B. Papadias, "Cost-efficient design of an energy-neutral uav-based mobile network," *IEEE Transactions on Communications*, vol. 70, no. 10, pp. 6890–6901, 2022.

[2] J. W. Röper, K. Fischer, M. C. Baumgarten, K. C. Thies, K. Hahnenkamp, and S. Fleßa, "Can drones save lives and money? an economic evaluation of airborne delivery of automated external defibrillators," *The European Journal of Health Economics*, vol. 24, no. 7, pp. 1141–1150, 2023.

[3] C. Cavalaris, "Challenges and opportunities for cost-effective use of unmanned aerial system in agriculture," *Unmanned Aerial Systems in Agriculture*, pp. 197–229, 2023.

[4] Z. Xiao, L. Zhu, Y. Liu, P. Yi, R. Zhang, X.-G. Xia, and R. Schober, "A survey on millimeter-wave beamforming enabled uav communications and networking," *IEEE Communications Surveys & Tutorials*, vol. 24, no. 1, pp. 557–610, 2021.

[5] E. Amaldi, A. Capone, and F. Malucelli, "Planning umts base station location: Optimization models with power control and algorithms," *IEEE Transactions on wireless Communications*, vol. 2, no. 5, pp. 939–952, 2003.

[6] M. Mozaffari, W. Saad, M. Bennis, and M. Debbah, "Efficient deployment of multiple unmanned aerial vehicles for optimal wireless coverage," *IEEE Communications Letters*, vol. 20, no. 8, pp. 1647–1650, 2016.

[7] S. Enayati, H. Saeedi, H. Pishro-Nik, and H. Yanikomeroglu, "Moving aerial base station networks: A stochastic geometry analysis and design perspective," *IEEE Transactions on Wireless Communications*, vol. 18, no. 6, pp. 2977–2988, 2019.

[8] R. Ghanavi, E. Kalantari, M. Sabbaghian, H. Yanikomeroglu, and A. Yongacoglu, "Efficient 3d aerial base station placement considering users mobility by reinforcement learning," in *2018 IEEE Wireless Communications and Networking Conference (WCNC)*. IEEE, 2018, pp. 1–6.

[9] P. Yu, J. Guo, Y. Huo, X. Shi, J. Wu, and Y. Ding, "Three-dimensional aerial base station location for sudden traffic with deep reinforcement learning in 5g mmwave networks," *International Journal of Distributed Sensor Networks*, vol. 16, no. 5, p. 1550147720926374, 2020.

[10] J. Qiu, J. Lyu, and L. Fu, "Placement optimization of aerial base stations with deep reinforcement learning," in *ICC 2020-2020 IEEE International Conference on Communications (ICC)*. IEEE, 2020, pp. 1–6.

[11] G. Geraci, A. Garcia-Rodriguez, M. M. Azari, A. Lozano, M. Mezzavilla, S. Chatzinotas, Y. Chen, S. Rangan, and M. Di Renzo, "What will the future of uav cellular communications be? a flight from 5g to 6g," *IEEE communications surveys & tutorials*, vol. 24, no. 3, pp. 1304–1335, 2022.

[12] B. Galkin, J. Kibilda, and L. A. DaSilva, "Deployment of uav-mounted access points according to spatial user locations in two-tier cellular networks," in *2016 Wireless Days (WD)*. IEEE, 2016, pp. 1–6.

[13] M. Ozturk, J. P. Nadas, P. H. Klaine, S. Hussain, and M. A. Imran, "Clustering based uav base station positioning for enhanced network capacity," in *2019 International Conference on Advances in the Emerging Computing Technologies (AECT)*. IEEE, 2020, pp. 1–6.

[14] J. Sun and C. Masouros, "Deployment strategies of multiple aerial bss for user coverage and power efficiency maximization," *IEEE Transactions on Communications*, vol. 67, no. 4, pp. 2981–2994, 2018.

[15] I. Valiulahi and C. Masouros, "Multi-uav deployment for throughput maximization in the presence of co-channel interference," *IEEE Internet of Things Journal*, vol. 8, no. 5, pp. 3605–3618, 2020.

[16] R. Cao, J. Ye, Q. You, J. Xu, Y. Wang, S. Jiang, and Y. Li, "Poster: A novel region-of-interest based uav planning strategy for mitigating urban peak demand," in *Proceedings of the Twenty-fourth International Symposium on Theory, Algorithmic Foundations, and Protocol Design for Mobile Networks and Mobile Computing*, 2023, pp. 300–301.

[17] E. Kalantari, I. Bor-Yaliniz, A. Yongacoglu, and H. Yanikomeroglu, "User association and bandwidth allocation for terrestrial and aerial base stations with backhaul considerations," in *2017 IEEE 28th Annual International Symposium on Personal, Indoor, and Mobile Radio Communications (PIMRC)*. IEEE, 2017, pp. 1–6.

[18] A. Al-Hourani, S. Kandeepan, and A. Jamalipour, "Modeling air-to-ground path loss for low altitude platforms in urban environments," in *2014 IEEE global communications conference*. IEEE, 2014, pp. 2898–2904.

[19] Y. Zeng and R. Zhang, "Energy-efficient uav communication with trajectory optimization," *IEEE Transactions on wireless communications*, vol. 16, no. 6, pp. 3747–3760, 2017.

[20] H. Müller, D. Palossi, S. Mach, F. Conti, and L. Benini, "Fünfiiber-drone: A modular open-platform 18-grams autonomous nano-drone," in *2021 Design, Automation & Test in Europe Conference & Exhibition (DATE)*. IEEE, 2021, pp. 1610–1615.

[21] "DJI Mavic 3 Pro - Specs - DJI — dji.com," https://www.dji.com/hk/mavic-3-pro/specs, [Accessed 10-10-2023].

[22] R. K. Jain, D.-M. W. Chiu, W. R. Hawe *et al.*, "A quantitative measure of fairness and discrimination," *Eastern Research Laboratory, Digital Equipment Corporation, Hudson, MA*, vol. 21, 1984.

[23] B. Zhou, A. Liu, and V. Lau, "Successive localization and beamforming in 5g mmwave mimo communication systems," *IEEE Transactions on Signal Processing*, vol. 67, no. 6, pp. 1620–1635, 2019.

[24] J.-N. Hwang, S.-R. Lay, and A. Lippman, "Nonparametric multivariate density estimation: a comparative study," *IEEE Transactions on Signal Processing*, vol. 42, no. 10, pp. 2795–2810, 1994.

[25] S. Zhang, H. Zhang, B. Di, and L. Song, "Cellular uav-to-x communications: Design and optimization for multi-uav networks," *IEEE Transactions on Wireless Communications*, vol. 18, no. 2, pp. 1346–1359, 2019.

[26] L. Reynaud, T. Rasheed, and S. Kandeepan, "An integrated aerial telecommunications network that supports emergency traffic," in *2011 The 14th International Symposium on Wireless Personal Multimedia Communications (WPMC)*. IEEE, 2011, pp. 1–5.